Elevated prolactin during pregnancy drives a phenotypic switch in mouse hypothalamic dopaminergic neurons

Article

Cell Reports

Elevated Prolactin during Pregnancy Drives a Phenotypic Switch in Mouse Hypothalamic Dopaminergic Neurons

Graphical Abstract

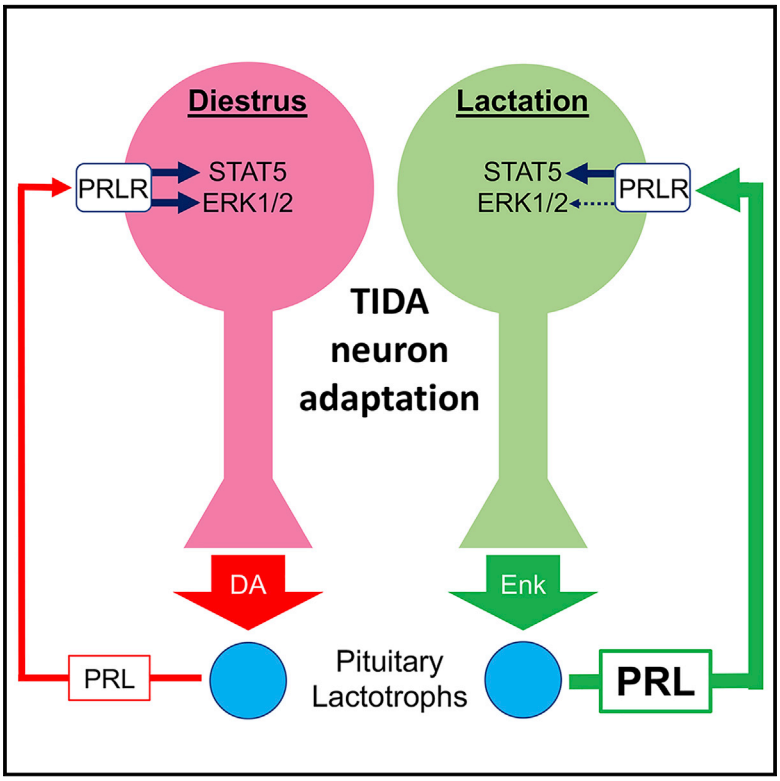

Highlights

- In lactation, TIDA neurons synthesize and release enkephalin in place of dopamine
- This switch in neurotransmitter is driven by neuronal prolactin receptors
- This adaptation coincides with altered prolactin signaling within TIDA neurons
- This promotes rather than inhibits prolactin secretion during lactation

Authors

Siew H. Yip, Nicola Romanò, Papillon Gustafson, ..., Patrice Mollard, David R. Grattan, Stephen J. Bunn

Correspondence

stephen.bunn@otago.ac.nz

In Brief

Pituitary prolactin secretion is inhibited by dopamine released by hypothalamic neurons. Yip et al. show that, during lactation, these TIDA neurons alter their response to prolactin and release enkephalin in place of dopamine. This mechanism promotes rather than inhibits prolactin secretion, supporting its elevation during lactation.

Yip et al., 2019, Cell Reports *26*, 1787–1799
February 12, 2019
https://doi.org/10.1016/j.celrep.2019.01.067

CellPress

Cell Reports
Article

Elevated Prolactin during Pregnancy Drives a Phenotypic Switch in Mouse Hypothalamic Dopaminergic Neurons

Siew H. Yip,[1,2] Nicola Romanò,[3] Papillon Gustafson,[1,2] David J. Hodson,[4,5] Eloise J. Williams,[1,2] Ilona C. Kokay,[1,2] Agnes O. Martin,[6] Patrice Mollard,[6] David R. Grattan,[1,2,7] and Stephen J. Bunn[1,2,8,*]
[1]Department of Anatomy, University of Otago, Dunedin 9054, New Zealand
[2]Centre for Neuroendocrinology, University of Otago, Dunedin 9054, New Zealand
[3]Centre for Discovery Brain Sciences, University of Edinburgh, Edinburgh EH8 9XD, Scotland
[4]Institute of Metabolism and Systems Research (IMSR) and Centre of Membrane Proteins and Receptors (COMPARE), University of Birmingham, Edgbaston B15 2TT, UK
[5]Centre for Endocrinology, Diabetes and Metabolism (CEDAM), Birmingham Health Partners, Birmingham B15 2TH, UK
[6]IGF, CNRS, INSERM, Université de Montpellier, Montpellier, France
[7]Maurice Wilkins Centre for Molecular Biodiscovery, Auckland 1010, New Zealand
[8]Lead Contact
*Correspondence: stephen.bunn@otago.ac.nz
https://doi.org/10.1016/j.celrep.2019.01.067

SUMMARY

Altered physiological states require neuronal adaptation. In late pregnancy and lactation, a sub-population of the mouse hypothalamic tuberoinfundibular dopaminergic (TIDA) neurons alters their behavior to synthesize and release met-enkephalin rather than dopamine. These neurons normally release dopamine to inhibit prolactin secretion and are activated by prolactin in a short-loop feedback manner. In lactation, dopamine synthesis is suppressed in an opioid-dependent (naloxone-reversible) manner, meaning that prolactin secretion is disinhibited. Conditional deletion of the prolactin receptor in neurons reveals that this change in phenotype appears to be driven by prolactin itself, apparently through an alteration in intracellular signaling downstream of the prolactin receptor that favors enkephalin production instead of dopamine. Thus, prolactin effectively facilitates its own secretion, which is essential for lactation and maternal behavior. These studies provide evidence of a physiologically important, reversible alteration in the behavior of a specific population of hypothalamic neurons in the adult brain.

INTRODUCTION

The anterior pituitary hormone, prolactin, mediates a wide range of physiological functions in addition to its archetypal lactotropic actions on the mammary gland (Bernichtein et al., 2010; Grattan, 2015; Grattan and Kokay, 2008). Within the brain, many of prolactin's actions facilitate maternal adaptation to pregnancy and behaviors conducive to the successful rearing of young (Brunton et al., 2008; Grattan and Kokay, 2008; Larsen and Grattan, 2012). In contrast to other pituitary hormones, endogenous prolactin secretion is high and predominately regulated by inhibitory tone from the hypothalamus, with disinhibition being a predominant mode of facilitating secretion. The anterior pituitary lactotrophs spontaneously release prolactin, which is tonically inhibited by dopamine secreted within the median eminence from the terminals of tuberoinfundibular dopaminergic (TIDA) neurons. In males and non-pregnant females, low circulating levels of prolactin are maintained by a "short-loop" negative feedback, in which prolactin directly interacts with the TIDA neurons to increase their firing rate and thus dopamine output (Brown et al., 2012, 2016; Freeman et al., 2000; Grattan et al., 2008; Lyons et al., 2012; Romanò et al., 2013).

During late pregnancy and lactation, circulating prolactin levels rise to support lactation and enable maternal behavioral adaptations (Arbogast and Voogt, 1996; Brisken et al., 1999; Grattan et al., 2008). For this to occur, the dopamine-mediated inhibitory tone upon the lactotrophs must be alleviated, despite the ongoing presence of elevated prolactin levels (and during late pregnancy, placental lactogen) in the circulation. A number of studies have suggested that the TIDA neurons become "refractory" to prolactin-mediated negative feedback during this time. For example, central administration of prolactin to non-pregnant female rats increases activity of tyrosine hydroxylase (TH), the rate-limiting step in dopamine synthesis, in the median eminence in non-pregnant rats but has no effect during lactation (Arbogast and Voogt, 1996; Demarest et al., 1983). Similarly, despite elevated prolactin levels during lactation, the rat arcuate nucleus shows reduced levels of both TH mRNA and TH protein, with an associated reduction in dopamine turnover and secretion at the median eminence (Andrews, 2005; Szabó et al., 2011). This downregulation of prolactin-induced dopamine synthesis and secretion during lactation does not arise from a reduction in prolactin receptor expression, with *in situ* hybridization revealing similar levels of prolactin receptor mRNA in the arcuate nucleus of non-pregnant and lactating rats and mice (Augustine et al., 2003; Brown et al., 2011; Kokay and Grattan, 2005). Most

strikingly, we have shown that prolactin-induced electrophysiological responses in TIDA neurons are unaltered between nonpregnant and lactating mice, although they now fail to synthesize and release dopamine (Romanò et al., 2013).

Intriguing observations made almost 25 years ago indicated that the opioid peptide enkephalin was expressed in the TIDA neurons during lactation (Ciofi et al., 1993; Merchenthaler, 1994). Because dopamine production is lost during this state, TIDA neurons may switch their phenotype from dopaminergic to enkephalinergic during lactation. Given that these neurons remain electrophysiologically responsive to prolactin during lactation (Romanò et al., 2013), it seems likely that enkephalin rather than dopamine may be the neurochemical output from these neurons at this time. Such a switch in output would be expected to have significant physiological consequences for the regulation of prolactin secretion during lactation.

The aim of this study was to test the hypothesis that prolactin feedback is responsible for the neurotransmitter switch in the TIDA neurons during late pregnancy and lactation. We also investigated the hypothesis that the transition from a dopaminergic to enkephalinergic phenotype involves an alteration in signal transduction pathways downstream of the prolactin receptor. Finally, we have investigated whether prolactin stimulates enkephalin release from the median eminence in the lactating mouse and the consequences of such action in terms of pituitary function. Together, the data suggest a profound change in the hypothalamic regulation of prolactin secretion during lactation, promoting a state of hyperprolactinemia. Essentially during this time, the short-loop negative feedback regulation of prolactin secretion switches to a condition where elevated prolactin facilitates its further secretion. Similar mechanisms may occur in other neuronal populations that undergo plasticity over lifespan in adults.

RESULTS

Met-Enkephalin Expression in the Arcuate Nucleus of the Mouse Is Increased during Lactation

There was no change in the number of TH-immunoreactive cells within the arcuate nucleus during late pregnancy and lactation (Figures 1A–1D). The level of *Th* mRNA expression in the arcuate nucleus was however markedly affected ($F [2,22] = 5.72$; $p < 0.01$; one-way ANOVA) such that it was significantly reduced during both late pregnancy and lactation compared to diestrus controls ($p < 0.05$; Tukey's multiple comparison test; Figure 1E). There was also a change in proenkephalin (*Penk*) mRNA expression during this time ($F [2,22] = 18.25$; $p < 0.0001$; one-way ANOVA), with its level increased during both late pregnancy and lactation compared to diestrus animals ($p < 0.0001$ and $p < 0.05$, respectively; Tukey's multiple comparison test; Figure 1J). The number of met-enkephalin immunoreactivity cells within the arcuate nucleus also increased during this time ($F [2,11] = 17.57$; $p < 0.001$; one-way ANOVA), being significantly greater during late pregnancy ($p < 0.001$) and lactation ($p < 0.001$) compared to diestrus controls (Tukey's multiple comparison test; Figures 1F–1I). The lactation-associated rise in met-enkephalin-expressing cell number was specific to the arcuate nucleus, with no significant change in met-enkephalin expression in the paraventricular nucleus and a significant decline in the dorsomedial hypothalamus (Figure S1).

During Lactation, the Majority of Met-Enkephalin-Expressing Cells in the Arcuate Nucleus Are Also Immunoreactive for Tyrosine Hydroxylase

In the dorsomedial arcuate nucleus, the primary location of the TIDA neurons (Freeman et al., 2000), the number of cells that were dual labeled for TH and met-enkephalin increased markedly during lactation (Figures 1K–1P). In diestrus animals, less than 10% of the met-enkephalin immunoreactive cells also expressed TH, whereas during lactation, this number had risen to about 80% ($p < 0.005$; Student's t test; Figure 1Q). It should be noted, however, that, even during lactation, although the number of dual-labeled cells was significantly increased ($p < 0.005$; Student's t test), they constituted only approximately one-third of all TH-positive neurons present in this region (34.8% ± 3.8%; Figure 1R).

The Lactation-Induced Increase in Met-Enkephalin and *Penk* mRNA Expression in TIDA Neurons Is Mediated by Prolactin

Alteration of prolactin levels significantly affected the number of met-enkephalin cells in the dorsomedial arcuate nucleus ($F [3,16] = 23.84$; $p < 0.0001$; one-way ANOVA; Figures 2A–2E). As expected, lactation increased the number of met-enkephalin immunoreactive cells compared to diestrus ($p < 0.0005$; Tukey's multiple comparison test; Figures 2A, 2C, and 2E). Suppressing prolactin levels in lactating mice with bromocriptine from 355.6 ± 62.7 ng/mL to 45.3 ± 9.1 ng/mL (compared to 18.2 ± 6.0 ng/mL during diestrus) significantly reduced the number of these cells ($p < 0.01$; Tukey's multiple comparison test) to approximately half that seen in untreated lactating animals (Figure 2B and 2E; 22.2 ± 2.1 cells per section in lactating animals falling to 10.9 ± 2.6 cells per section following treatment with bromocriptine). Furthermore, maintaining serum prolactin levels in bromocriptine-treated lactating mice with ovine prolactin (245.8 ± 69.1 ng/mL) prevented this decrease in number of met-enkephalin-expressing cells such that it was similar to that seen during lactation (30.4 ± 2.1 cells per section; Figures 2D and 2E). *In situ* hybridization revealed that the number of cells in the arcuate nucleus expressing *Penk* mRNA during lactation increased more than 10-fold compared to diestrus animals (1.6 ± 0.5 to 20.2 ± 2.0 cells per section; Figures 2F–2H). Similarly, the number of cells expressing *Penk* mRNA, which was low in lactating animals 24 h after pup withdrawal, was significantly increased when the circulating concentration of prolactin was increased to greater than 100 ng/mL by osmotic pump infusion of exogenous prolactin (2.7 ± 1.2 to 11.8 ± 4.2 cells per section; Figures 2I–2K).

The Lactation-Induced Increase in Met-Enkephalin and *Penk* mRNA Expression in the TIDA Neurons Is Dependent on a Neuronal Prolactin Receptor

The observations above suggest that prolactin acts on TIDA neurons during late pregnancy or lactation to promote met-enkephalin expression. This concept was confirmed by data obtained from $PRLR^{lox/lox}$/CamK-Cre mice, which lack prolactin receptors in forebrain neurons, including TIDA neurons (Brown et al., 2016).

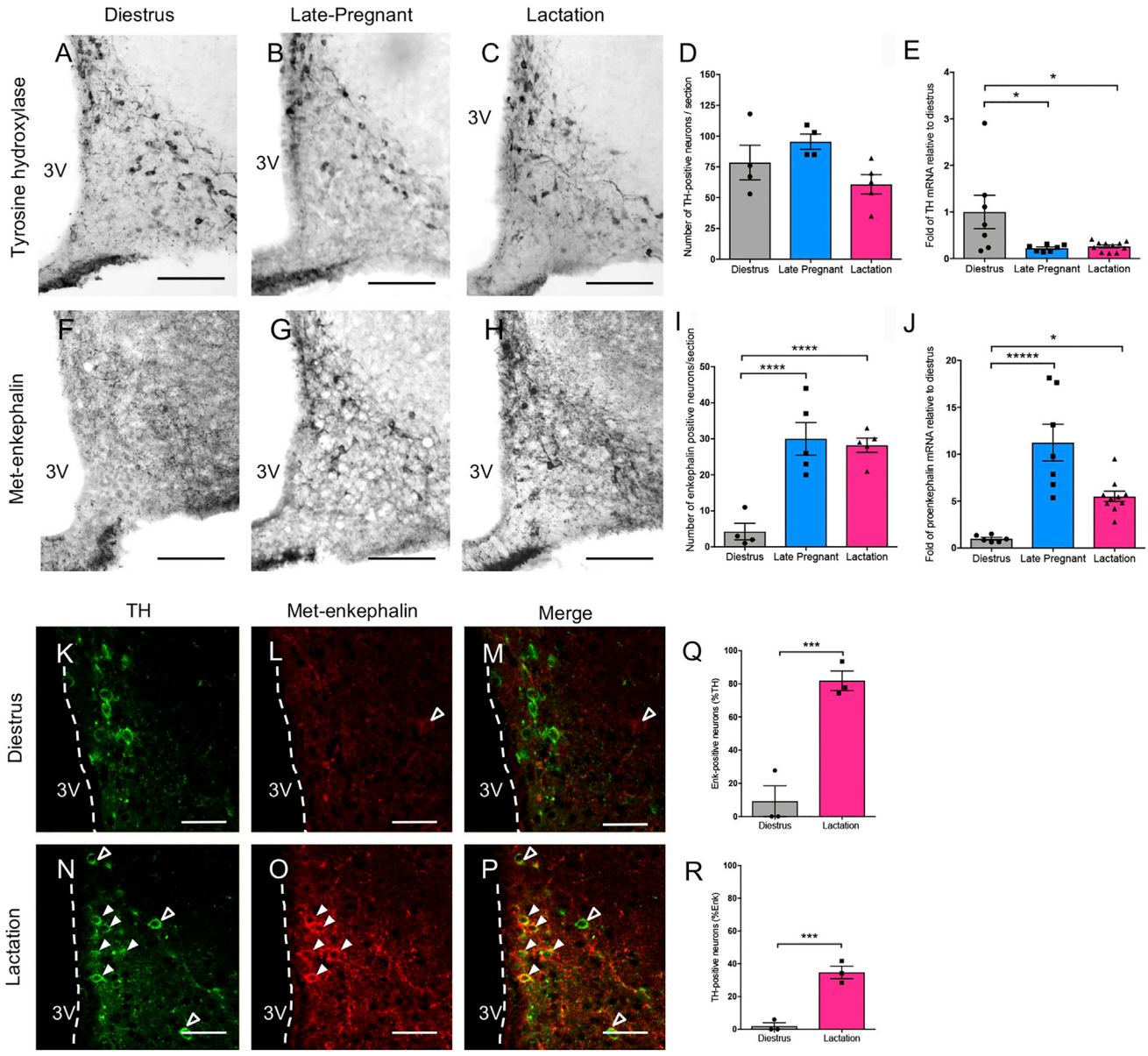

Figure 1. Met-Enkephalin Expression in Tyrosine-Hydroxylase-Positive Neurons within the Arcuate Nucleus Is Increased during Lactation

(A–J) Representative images of arcuate nucleus sections showing tyrosine hydroxylase (TH) (A–C) and met-enkephalin (F–H) immunoreactive cells in diestrus (A and F), late pregnant (B and G), and lactating (C and H) mice. Quantification of the number of TH and met-enkephalin immunoreactive cells is shown in (D) and (I), respectively, and is presented as the mean ± SEM per section (data analyzed by one-way ANOVA followed by Tukey's multiple comparison test; n = 4 or 5). *Th* and *Penk* mRNA expression in the arcuate nucleus is shown in (E) and (J), respectively, with levels in late pregnancy and lactation presented relative to those found during diestrus (data analyzed by one-way ANOVA followed by a Tukey's multiple comparison test; n = 6–11).

(K–P) Representative confocal images of dorsomedial arcuate nucleus sections showing TH (green), met-enkephalin (red) immunoreactive cells, and merged images of diestrus (K–M) and lactating (N–P) mice. Filled arrowheads indicate TH immunoreactive cell bodies co-labeled with met-enkephalin, and open arrowheads indicate either TH or met-enkephalin immunoreactive cell bodies, which are not dual labeled.

(Q) The percentage of met-enkephalin immunoreactive cells that were also stained for TH in the dorsomedial arcuate nucleus.

(R) The percentage TH immunoreactive cells in the same region that were also stained for met-enkephalin.

Data represent the mean ± SEM (n = 3 mice), and statistical analysis was performed using an unpaired Student's t test. 3V, third ventricle. Scale bars: (A–C and F–H) 100 μm and (K–P) 30 μm. *p < 0.05, ***p < 0.005, ****p < 0.001, and *****p < 0.0001.

Despite being hyperprolactinemic, due to the lack of prolactin feedback on TIDA neurons, these animals could become pregnant but often failed to nurse their pups (Brown et al., 2016). Hence, all investigations were conducted on day 18 of pregnancy. Both reproductive ($F [1,17] = 9.03$; $p < 0.01$; two-way ANOVA) and genetic ($F [1,17] = 12.84$; $p < 0.005$; two-way

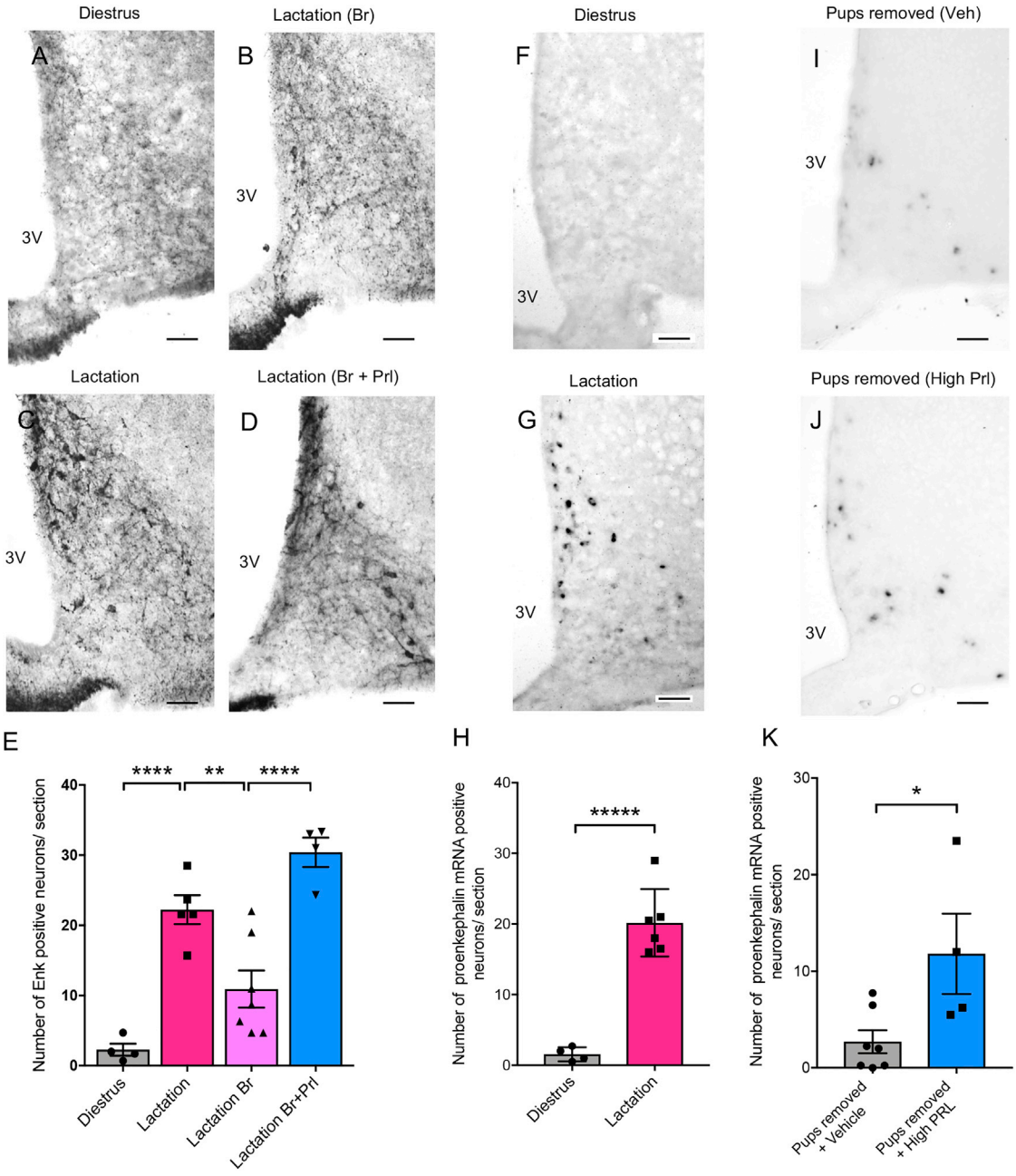

Figure 2. The Lactation-Induced Increase in Met-Enkephalin and *Penk* mRNA Expression in TIDA Neurons Is Mediated by Prolactin

(A–D) Representative images of met-enkephalin immunoreactivity in the dorsomedial arcuate nucleus of diestrus (A), lactating (C), and bromocriptine-treated lactating mice with (D) or without (B) ovine prolactin replacement.

(E) Quantitation of the number of met-enkephalin immunoreactive cells per section under each condition. Data represent the mean ± SEM, and statistical analysis was conducted using one-way ANOVA followed by a Tukey's multiple comparison test (n = 4–7).

(F–H) *Penk* mRNA expression in diestrus (F) and lactating (G) mice. Quantitation of the number of *Penk*-mRNA-positive cells per section under each condition is presented in (H). Data represent the mean ± SEM, and statistical analysis was performed using an unpaired Student's t test (n = 4–6 mice).

(I–K) *Penk* mRNA in lactating animals that have undergone pup-withdrawal with (J) or without (I) prolactin replacement (high prolactin defined as >100 ng/mL). Quantitation of the number of *Penk*-mRNA-positive cells per section under each condition is presented in (K).

Data represent the mean ± SEM, and statistical analysis was conducted using one-way ANOVA followed by a Tukey's multiple comparison test (n = 4–7). Br, bromocriptine; Prl, ovine prolactin; 3V, third ventricle. Scale bars: 50 μm. *$p < 0.05$, **$p < 0.01$, ****$p < 0.0005$, and *****$p < 0.0001$.

ANOVA) status significantly influenced the number of met-enkephalin-positive cells in the arcuate nucleus, with a significant interaction between the two factors ($F [1,17] = 13.9$; $p < 0.005$; two-way ANOVA; Figures 3A–3E). In contrast to age-matched $PRLR^{lox/lox}$ Cre-negative controls, the prolactin receptor-deleted animals showed no increase in arcuate nucleus met-enkephalin immunoreactivity in late pregnancy, with the number of met-enkephalin immunoreactive cells remaining unchanged from those in the non-pregnant state (3.9 ± 0.8 and 4.6 ± 2.1 cells per section, respectively; Figures 3C–3E). As can be seen in Figures 3F–3J, deletion of the neuronal prolactin receptor had an essentially identical effect on *Penk* mRNA expression in the arcuate nucleus with the rise in the number of *Penk*-mRNA-positive cells during late pregnancy being abolished in animals lacking the neuronal prolactin receptor ($F [1,19] = 109.1$; $p < 0.0001$; two-way ANOVA; Figure 3J).

Prolactin-Receptor-Mediated Signaling in the TIDA Neurons Is Altered during Lactation

If, as our data suggest, prolactin stimulation of TIDA neurons can drive met-enkephalin expression during late pregnancy and lactation but drives dopamine synthesis and secretion at other times, this may indicate a pregnancy-induced change to the signal-transduction pathways mediating prolactin action in the TIDA neurons. Prolactin receptor stimulation activates both the signal transducer and activator of transcription 5 (STAT5) and extracellular-signal-regulated 1/2 (ERK1/2) pathways. Immunohistochemistry revealed that reproductive status has a significant effect on the number of TH-immunoreactive cells expressing activated (tyrosine phosphorylated) STAT5 (pSTAT5) ($F [2,15] = 98.82$; $p < 0.0001$; two-way ANOVA) and that this was significantly influenced by experimental manipulation of prolactin levels ($F [2,15] = 12.47$; $p < 0.001$; two-way ANOVA). During diestrus, slightly less than half (46.8% ± 7.9%) of the TH immunoreactive cells in the dorsomedial arcuate displayed nuclear pSTAT5 labeling (Figures 4A and 4G). As expected, due to the elevated circulating prolactin in lactating mice, this number significantly increased to 81.6% ± 4.0% ($p < 0.01$; Tukey's multiple comparisons test; Figures 4D and 4G). Suppression of prolactin secretion with bromocriptine essentially abolished pSTAT5 immunoreactivity in both diestrus and lactating animals (Figures 4B, 4E, and 4G). Acute administration of exogenous prolactin to bromocriptine-treated animals resulted in a significant, and similar, increase in the number of TH-pSTAT5 dual-labeled cells in both diestrus and lactating animals ($p < 0.0001$; Tukey's multiple comparisons test in both cases) compared to that seen following bromocriptine treatment (Figures 4C, 4F, and 4G). The data in Figure 4 also show that reproductive status alters the number of TH-immunoreactive cells expressing phosphorylated ERK1/2 (pERK1/2) ($F [2,19] = 13.45$; $p < 0.0003$; two-way ANOVA) and that this was significantly influenced by experimental manipulation of prolactin levels ($F [2,19] = 26.29$; $p < 0.0001$; two-way ANOVA). During diestrus, a lower percentage of TH-immunoreactive cells were dual labeled for pERK1/2 compared to those expressing pSTAT5 (compare Figure 4G with 4N). The number of pERK1/2-stained TH cells increased markedly in lactation, rising approximately four-fold from 4.8% ± 0.5% in diestrus to 21.6% ± 4.5% in lactation ($p < 0.01$; Tukey's multiple comparisons test; Figures 4H, 4K, and 4N). Bromocriptine treatment did not affect pERK1/2 expression in diestrus animals but abolished the lactation-associated rise (Figures 4I, 4L, and 4N). Although acute treatment with exogenous prolactin to bromocriptine-treated animals stimulated an almost 10-fold increase in the number of TH-positive cells also expressing pERK1/2 in diestrus mice ($p < 0.001$; Tukey's multiple comparisons test; Figures 4J and 4N), it was without a significant effect on lactating animals (Figures 4M and 4N). The effect of acute prolactin treatment on bromocriptine-treated animals was also investigated using western blot analysis of arcuate nucleus micro-punch samples. In agreement with the immunohistochemical data described above, western blot analysis confirmed that acute prolactin treatment (20 min) increased pSTAT5 levels in both diestrus and lactating mice, but the pERK1 and pERK2 responses were lost in the latter (Figure S2).

Prolactin Stimulates the Release of Met-Enkephalin from the Median Eminence of the Lactating Mouse, which May Reduce the Activity of Tyrosine Hydroxylase

Met-enkephalin expression in TIDA neurons during late pregnancy and lactation may lead to its release at the median eminence. To examine this possibility, brain slices at the level of the arcuate nucleus from lactating mice were exposed to saline or prolactin for 30 min and then fixed and dual stained for met-enkephalin and TH. Under basal conditions, strong met-enkephalin immunoreactivity was closely associated with the TH-expressing external zone of the median eminence (Figure 5A, left panels). After prolactin application, the intensity of the TH staining remained unchanged, whereas met-enkephalin immunoreactivity was significantly reduced compared to that seen in slices treated with saline alone (Figures 5A and 5B). Because these data suggest that prolactin may stimulate met-enkephalin release from nerve terminals in the median eminence of lactating mice, we investigated two possible physiological targets for this opioid peptide: first, the TIDA neurons themselves, and second, the anterior pituitary lactotrophs. In the former experiments, pregnant mice were treated with the opioid receptor antagonist, naloxone, from late gestation to day 10 of lactation. Western blot analysis of hypothalamic tissue from these animals showed a significant increase in the level of activated TH (as indicated by its phosphorylation on serine-40) compared to that seen in lactating animals treated with saline only (Figure 5C; $p < 0.05$; Student's t test). These data are consistent with a tonic opioid-mediated inhibition of TH phosphorylation in the TIDA neurons during lactation, which would effectively reduce the activity of this enzyme and thus suppress the production of dopamine.

Met-Enkephalin Increases Ca^{2+} Signaling and Prolactin Secretion from Pituitary Lactotrophs of Lactating Mice

To determine the effect of met-enkephalin on the lactotrophs, pituitary slices from prolactin-DsRed animals (He et al., 2011; Hodson et al., 2012) were loaded with the Ca^{2+} indicator Fura-2 and the Ca^{2+} responses measured. In approximately one-third of the cells, a 15-min treatment with met-enkephalin (500 nM) induced a strong increase in the Ca^{2+}-spiking activity

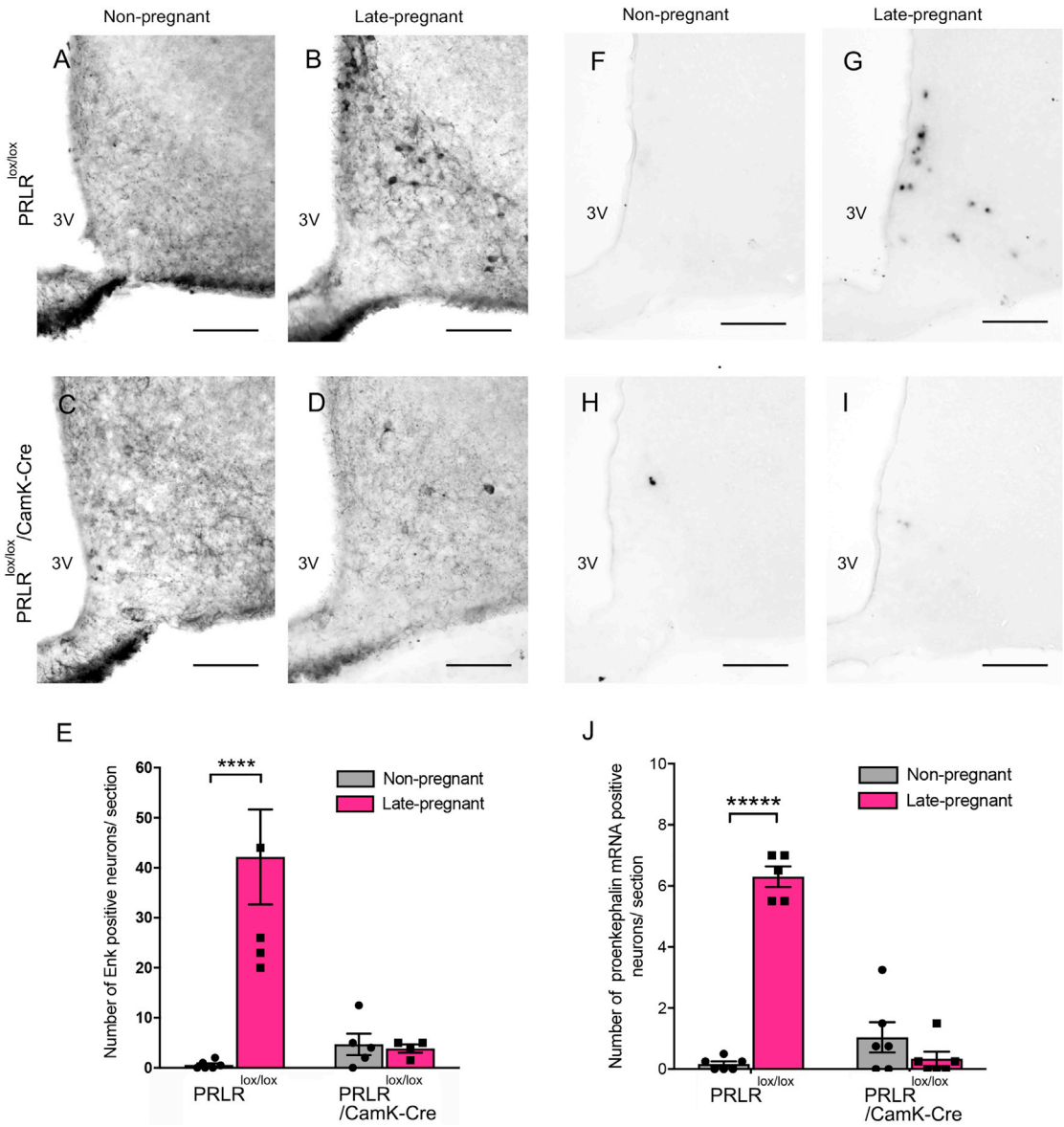

Figure 3. The Lactation-Induced Increase in Met-Enkephalin and *Penk* mRNA Expression in the TIDA Neurons Is Dependent on a Neuronal Prolactin Receptor

(A–D) Representative images of met-enkephalin immunoreactivity in the arcuate nucleus of $PRLR^{lox/lox}$ (A) and $PRLR^{lox/lox}$/CamK-Cre (C) non-pregnant mice, and $PRLR^{lox/lox}$ (B) and $PRLR^{lox/lox}$/CamK-Cre (D) late-pregnant mice.

(F–I) Representative images of *Penk* mRNA expression in the arcuate nucleus of $PRLR^{lox/lox}$ (F) and $PRLR^{lox/lox}$/CamK-Cre (H) non-pregnant mice, and $PRLR^{lox/lox}$ (G) and $PRLR^{lox/lox}$/CamK-Cre (I) late pregnant mice.

Quantitation of the number of met-enkephalin immunoreactive and *Penk*-expressing cells per section under each of the above conditions is shown in (E) and (J), respectively. Data represent the mean ± SEM, and statistical analysis was performed using two-way ANOVA followed by a Tukey's multiple comparison test, n = 4–6. Grey columns, diestrus; pink columns, lactating. Scale bars: 75 μm. ****$p < 0.0005$ and *****$p < 0.0001$.

of the lactotroph population (n = 327/957 responsive lactotrophs in 7 slices from 3 animals; Figures 6A–6C). Analysis of the frequency domain using short-time Fourier transform confirmed the presence of increased power at higher frequency ranges during the application of met-enkephalin, indicating a statistically significant effect of treatment on lactotroph Ca^{2+}-spiking activity (Figures 6D and 6E). To determine whether this corresponded to an increase in lactotroph output, hemipituitary explants from lactating animals were incubated for 10 min with met-enkephalin (500 nM) followed by measurement of prolactin concentrations in the medium by ELISA. Met-enkephalin induced a moderate but significant increase in prolactin secretion compared to controls (Figure 6F; $p < 0.05$; n = 4–6 pituitaries).

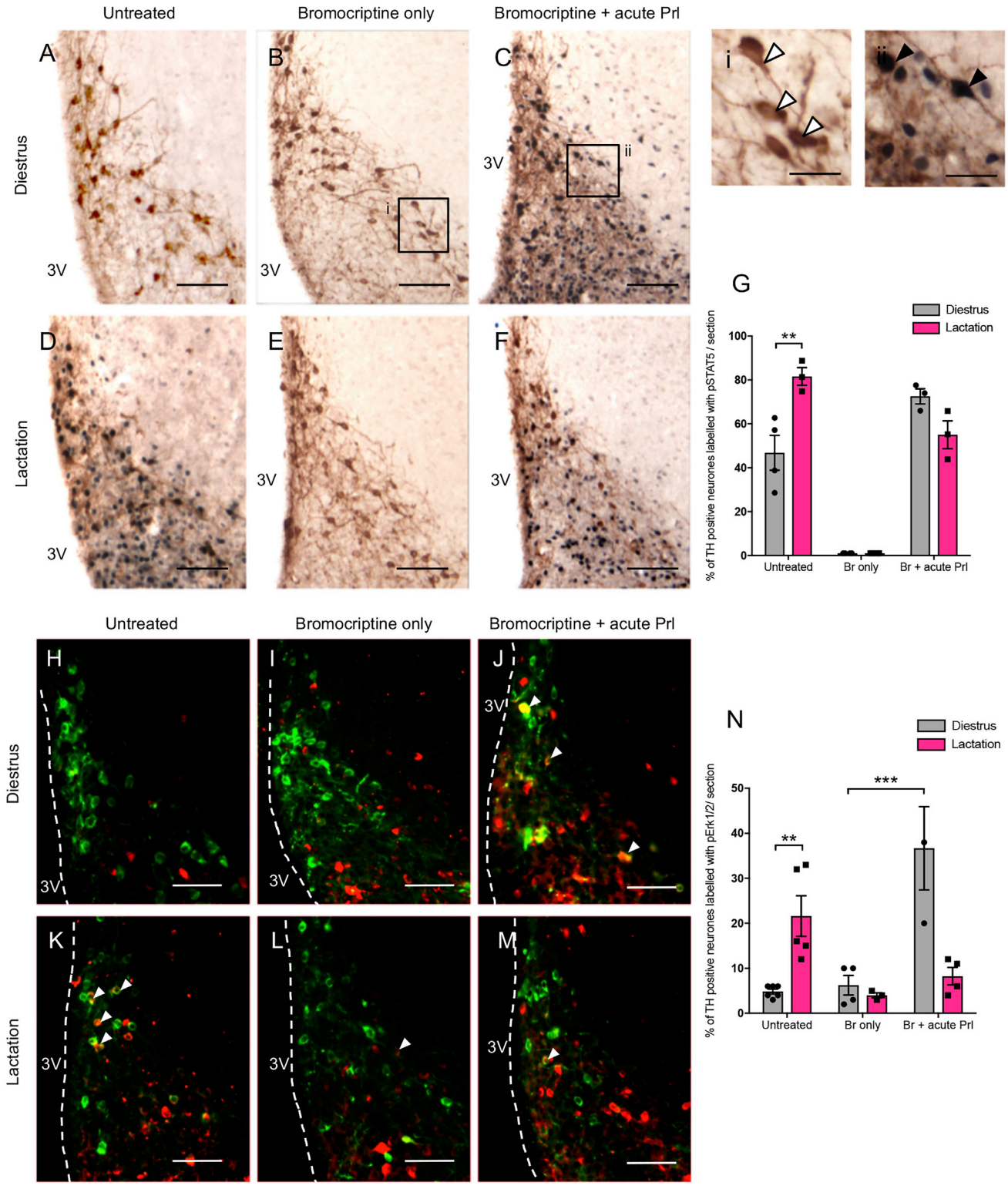

Figure 4. Prolactin-Receptor-Mediated Signaling in the TIDA Neurons Is Altered during Lactation

(A–F) Representative images of the dorsomedial arcuate nucleus showing TH (brown cytoplasmic staining) and pSTAT5 (black nuclear staining) immunoreactivity in diestrus and lactating mice. Diestrus animals (A) received bromocriptine pre-treatment with (C) or without (B) acute (20 min) prolactin injection. Matched images

(legend continued on next page)

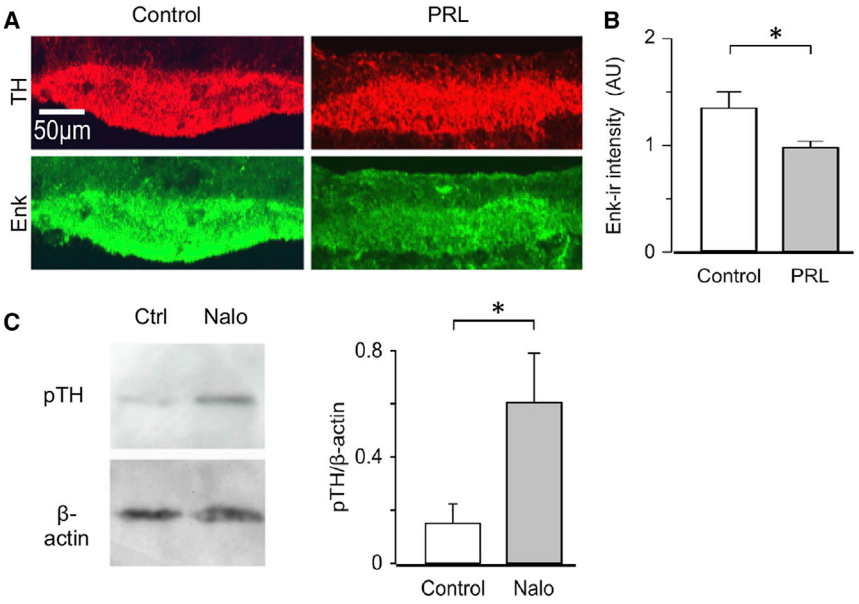

Figure 5. Prolactin Stimulates the Release of Met-Enkephalin from the Median Eminence of the Lactating Mouse, which May Reduce the Activity of Tyrosine Hydroxylase

(A) Representative images of the median eminence from lactating mice, showing prolactin-induced secretion of met-enkephalin. The intensity of TH immunoreactivity (red) was not affected by a 30-min incubation with prolactin (upper images), whereas met-enkephalin immunoreactivity (green) was reduced (lower images).

(B) Quantification of the met-enkephalin immunoreactivity in the median eminence (normalized for TH immunoreactivity) with or without prolactin (PRL) stimulation. Data represent the mean ± SEM (*$p < 0.05$; unpaired Student's t test; n = 5 from 3 animals).

(C) Representative western blot and quantitation of serine-40 phosphorylated TH (pTH) and β-actin content in the median eminence and arcuate nucleus of control (Ctrl) and naloxone-treated (Nalo) lactating mice (10 mg/kg).

Data represent the mean ± SEM (*$p < 0.05$; unpaired Student's t test; n = 4 controls, 5 naloxone). Scale bar: 50 μm.

DISCUSSION

Physiological hyperprolactinemia is essential for successful lactation, because it establishes milk production and facilitates adaptation of maternal physiology and behavior (Grattan et al., 2008; Grattan and Le Tissier, 2015). Elevation of circulating prolactin concentration is achieved, at least in part, by a relaxation of the negative-feedback pathway by which prolactin suppresses its own secretion through promoting dopamine release from the TIDA neurons. We have shown previously that, although the TIDA neurons reduce dopamine synthesis and release during lactation, they remain electrophysiologically responsive to prolactin (Romanò et al., 2013). The physiological significance of this persistent prolactin response in the absence of a dopaminergic output has been unknown. We report here that during late pregnancy and lactation, a sub-population of TIDA neurons undergoes a prolactin-dependent transition from a dopaminergic to enkephalinergic phenotype. Prolactin-induced stimulation of met-enkephalin release from the TIDA neurons during lactation may promote further prolactin secretion from the pituitary, through either suppression of dopamine synthesis and release or a direct stimulatory action on the lactotrophs. Thus, a sub-population of the TIDA neurons appear to undergo a phenotypic switch during late pregnancy and lactation, converting a dopaminergic short-loop negative feedback system into one using met-enkephalin to induce a positive stimulus for prolactin release. Such neurotransmitter switching is becoming increasingly recognized as a form of neuronal plasticity (Spitzer, 2017). Our proposed model of TIDA neuron plasticity during late pregnancy and lactation is summarized diagrammatically in Figure 7.

Lactation was associated with a decrease in *Th* mRNA and an increase in *Penk* mRNA within the arcuate nucleus. The observation that these changes were already present in late pregnancy suggests they result from hormonal as well as suckling-induced neuronal signaling to the TIDA neurons (Berghorn et al., 2001; Szabó et al., 2011; Wang et al., 1993). The absence of a corresponding reduction in the level of TH protein indicates the complex nature of TH regulation (Kumer and Vrana, 1996) but is consistent with previous findings showing that reduced dopamine synthesis in this region results from lower levels of the activated TH (serine-40 phosphorylated) rather than total enzyme (Romanò et al., 2013). Dual labeling for TH and met-enkephalin immunoreactivity indicated that approximately one-third of the dopaminergic neurons, presumed to be TIDA neurons, also expressed met-enkephalin during lactation. Although this is a marked rise from the situation in diestrus animals, it contrasts with findings in the lactating rat, where almost all TIDA neurons expressed enkephalin (Merchenthaler, 1994; Merchenthaler et al., 1995). It should be noted, however, that, unlike the data

from lactating animals are presented in (D), (E), and (F), respectively. (i) and (ii) present higher-magnification images of the boxed areas in (B) and (C), showing single-labeled TH cells (white arrowheads) and dual-labeled TH/pSTAT5 cells (black arrowheads).

(G) The percentage of TH immunoreactive cells dual labeled with pSTAT5 under each of the six experimental conditions is presented.

(H–M) Representative epifluorescent images of the dorsomedial arcuate nucleus showing TH (green) and pERK1/2 (red) immunoreactivity in diestrus and lactating mice. Diestrus animals (H) received bromocriptine pre-treatment with (J) or without (I) acute (20 min) prolactin injection. Matched images from lactating animals are presented in (K), (L), and (M), respectively.

(N) The percentage of TH immunoreactive cells dual labeled with pERK1/2 under each of the six conditions is presented.

All data represent the mean ± SEM, and statistical analysis was performed using two-way ANOVA followed by Tukey's multiple comparison test (n = 3–6). Grey columns, diestrus; pink columns, lactating; scale bars represent 50 μm. In (G), ** indicated $p < 0.01$, and in (N), **$p < 0.01$ compared diestrus controls and ***$p < 0.001$ compared to bromocriptine-treated diestrus animals.

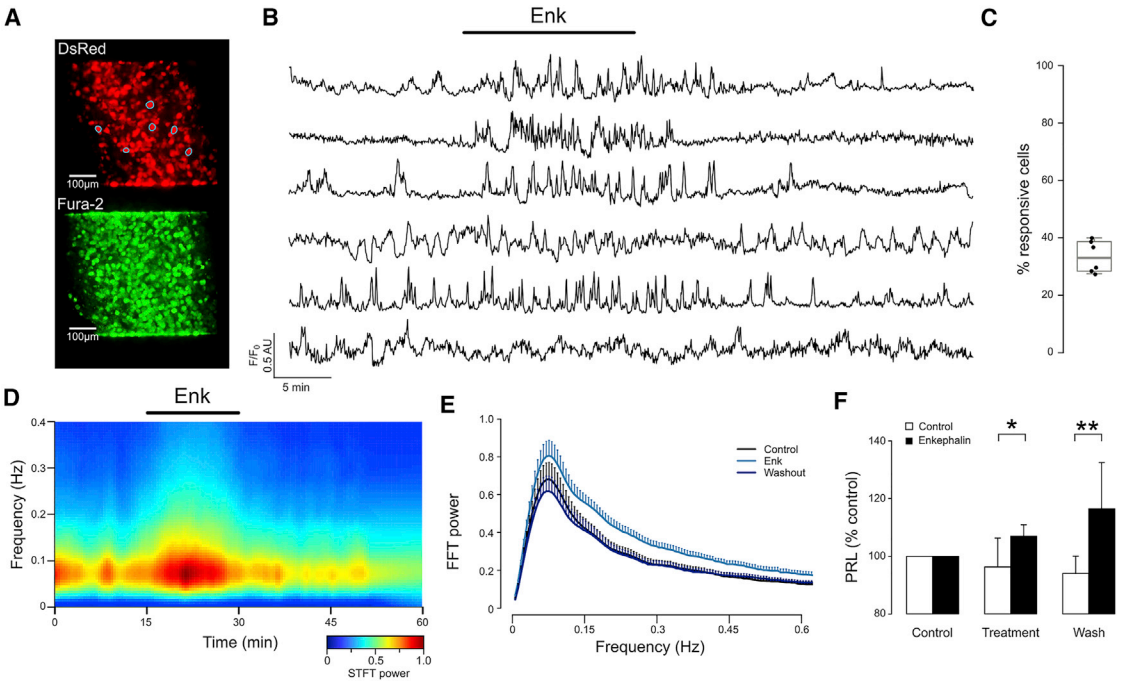

Figure 6. Met-Enkephalin Increases Ca^{2+} Signaling and Prolactin Secretion from Pituitary Lactotrophs of Lactating Mice

(A) Representative image of Fura-2 fluorescence in an acute pituitary slice from PRL-DsRed mouse.

(B) Example traces for the 6 lactotrophs (circled in A) treated for 15 min with met-enkephalin (500 nM; indicated by the bar).

(C) 15 min treatment with met-enkephalin induced increased Ca^{2+} spiking in approximately one-third of the lactotrophs (n = 327/957 responsive lactotrophs in 7 slices from 3 animals).

(D) Average STFT spectrogram for the Ca^{2+} recordings of cells responsive to Enk stimulation, showing an increase in FFT power throughout the frequency range analysed during the Enk treatment (black bar).

(E) Average frequency spectrum (shown as average ± SEM) in the 15 min preceding (black line), during (light blue line) or after (dark blue line) Enk exposure (***$p < 0.0001$, control versus Enk and wash versus Enk, mixed effect model).

(F) Met-enkephalin (500 nM for 15 min) significantly increased PRL secretion from hemi-pituitary explants compared to those maintained in media alone (*$p < 0.05$; **$p < 0.01$; unpaired Student's t test; n = 4–6 pituitaries). Open columns, saline treated; filled columns, enkephalin treated.

reported here, the antibody used in these earlier studies does not distinguish between met- and leu-enkephalin. Although the actual percentage of dual-labeled cells may be influenced by species or methodological differences, our current data are consistent with growing recognition that the TIDA neurons may not represent a homogeneous population. Arcuate dopamine neurons have been found, for example, to exist in distinct groups in terms of their electrophysiological characteristics (Liang and Pan, 2011; Romanò et al., 2013; Zhang and van den Pol, 2015), expression of potential co-transmitters (Brown et al., 2016), and catecholamine-synthesizing enzymes and transporters (Battaglia et al., 1995; Ugrumov, 2009). Most strikingly, recent studies using single-cell genetic profiling have identified up to six subtypes of dopaminergic neurons in this region (Campbell et al., 2017; Romanov et al., 2017). It is currently unknown whether the met-enkephalin-expressing TIDA neurons are coincident with one of these identified sub-populations, but the observation that essentially all TH-immunoreactive nerve terminals in the mouse median eminence also stained for enkephalin during lactation (Ciofi et al., 1993) suggests they may preferentially target the median eminence and thereby represent true neuroendocrine neurons.

The induction of met-enkephalin in the TIDA neurons was driven by prolactin and was lost following pharmacological suppression of prolactin during lactation or in the absence of prolactin receptors in the brain. These observations are supported by previous findings in the rat that indicated that prolactin can induce enkephalin expression in TIDA neurons during lactation (Merchenthaler et al., 1995; Nahi and Arbogast, 2003). The fact that the changes were initiated during pregnancy suggests that placental lactogen is likely to be the major factor acting through the prolactin receptor to mediate this effect (see Figure 7). It should be noted that, although the D2 agonist bromocriptine was employed in these studies to suppress prolactin release from the pituitary, it may also target other D2 receptors, including dopaminergic autoreceptors expressed on the TIDA neurons, which have been reported to provide an ultrafast negative feedback (Stagkourakis et al., 2016). The profile of *Penk* mRNA expression, determined by *in situ* hybridization, paralleled the above immunohistological observations, with the lactation-associated rise in number of *Penk*-mRNA-positive cells within the arcuate nucleus being reversed by prolactin depletion (following pup-withdrawal) and partially restored by prolactin replacement. Similarly,

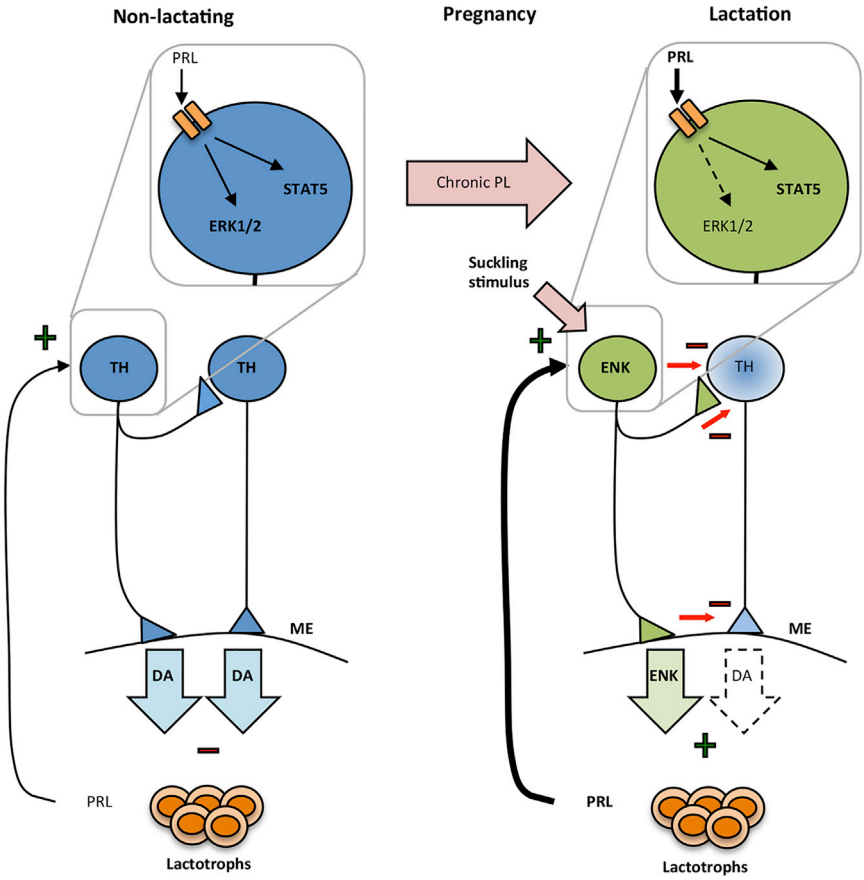

Figure 7. Diagrammatic Summary Depicting the Lactation-Induced Change in the TIDA Neuron Phenotype

During a non-lactating state, the TIDA neurons respond to prolactin by releasing dopamine (DA) (light blue arrow) into the portal blood at the median eminence (ME), which in turn inhibits prolactin secretion from lactotrophs. Chronic exposure to the prolactin agonist placental lactogen during pregnancy results in an alteration in the prolactin receptor signaling pathway, which supports met-enkephalin (ENK, light green arrow) expression in a subpopulation of the TIDA neurons. Suckling-induced activation of these neurons results in the release of the opioid, which acts on neighboring TIDA neurons to suppress dopamine synthesis (red arrows) and secretion at the median eminence (broken arrow), and directly on the lactotrophs, increasing prolactin secretion. As a result of this lactation-induced change in the TIDA neuron phenotype, the original prolactin-mediated negative feedback loop has been effectively converted to one of positive feedback.

depletion of neuronal prolactin receptors also prevented a lactational rise in the number of Penk-mRNA-expressing cells.

The ability of prolactin to switch from driving a dopaminergic to an enkephalinergic output from the TIDA neurons during late pregnancy and lactation may result from a modification to the intracellular signaling profile activated by its receptor. The physiological trigger for such a change is likely to arise from the dramatic pregnancy-specific alteration in the pattern of prolactin receptor activation occurring at this time, with high levels of placental lactogen providing a prolonged, chronic stimulus as distinct from the short-term, phasic patterns of prolactin secretion seen in early pregnancy. Although prolactin receptors are coupled to multiple intracellular signals, we focused on the two major pathways mediated by pSTAT5 and pERK1/2, respectively (Freeman et al., 2000). As expected, the elevation of endogenous prolactin during lactation significantly increased the percentage of dopaminergic (TH-expressing) cells also labeled with pSTAT5 or pERK1/2 compared to the levels seen in diestrus animals when prolactin is low. Interestingly, if endogenous prolactin levels were first suppressed with bromocriptine, diestrus and lactating animals exhibited a similar pSTAT5 responsiveness to the injection of exogenous prolactin, but the pERK1/2 signal was lost in the latter group. This conclusion was supported by parallel western blot analysis, which also showed preservation of the prolactin-induced pSTAT5 response but loss of the pERK signaling during lactation. This suggests that, although prolactin receptor coupling to the pSTAT5 pathway is unchanged between the two physiological states, its ability to signal via pERK1/2 has been markedly downregulated in the lactating mice. It should be noted that, although pSTAT5 is primarily a transcription factor, pERK is a multifunction protein kinase with both nuclear and cytoplasmic targets. Although the role of a diminished pERK1/2 response in prolactin-mediated met-enkephalin expression is unknown, it is consistent with a reduction in the phosphorylation of TH and thus a fall in the dopamine-synthesizing capacity of these neurons.

The proposal that TIDA neurons release enkephalin rather than dopamine during lactation is supported by evidence that increased opioid signaling may underlie lactational hyperprolactinemia (Arita and Kimura, 1988; Chihara et al., 1978; Meltzer et al., 1978; Rivier et al., 1977). Most notably, immunoneutralization of endogenous opioids or the administration of naloxone (or mu- or kappa-selective opioid receptor antagonists) suppresses both the antepartum prolactin surge and suckling-induced prolactin secretion in rats (Andrews and Grattan, 2002; Arbogast and Voogt, 1998; Callahan et al., 2000). Furthermore, both mu and kappa opioid receptor mRNA is expressed in the medial basal hypothalamus (Tavakoli-Nezhad and Arbogast, 2010) and lactation is associated with increased enkephalin immunoreactivity in the median eminence (Ciofi et al., 1993; Merchenthaler, 1994). Although the physiological targets of secreted opioid peptide have yet to be determined, close appositions between met-enkephalin fibers and dopaminergic neurons in the median eminence and arcuate nucleus suggest a possible opioid action on the TIDA neurons (Magoul et al., 1993, 1994; Mansour et al., 1993; Zhang and van den Pol, 2015), a possibility supported by electrophysiological data that opioid receptor agonists inhibit TIDA neuron activity (Zhang and van den Pol, 2015).

Similarly, *in vivo* and *in vitro* studies have shown that enkephalin inhibits dopamine turnover in the median eminence (Arita and Kimura, 1988; Ferland et al., 1977), an observation consistent with the data presented here that naloxone increases the serine-40 phosphorylation, and thus activity, of TH in the arcuate nucleus of the lactating mouse. These results suggest that, during late pregnancy and lactation, prolactin- or placental-lactogen-induced met-enkephalin released from TIDA neurons may exert autocrine signaling to suppress dopamine output and thus disinhibit the lactotrophs, allowing increased prolactin release from the pituitary.

The data presented in Figure 6 suggest that prolactin may stimulate met-enkephalin release from the median eminence, from where it may potentially access and target the pituitary lactotrophs. Although this interpretation of these immunohistochemical data is consistent with our overall hypothesis, it is important to stress that this approach does not directly measure enkephalin release and should therefore be interpreted conservatively. Further verification using a more direct quantitative approach will be required to confirm this.

Such a proposal is, however, supported by the presence of opioid receptors on a subset of anterior pituitary cells in the rat (Carretero et al., 2004) and evidence that met-enkephalin either promotes prolactin secretion (Carretero et al., 1992) or overcomes its suppression by dopamine (Enjalbert et al., 1979). Our current data extend these observations by showing that met-enkephalin directly increases Ca^{2+} signaling in a sub-population of lactotrophs in the intact mouse pituitary gland and that this response is concurrent with increased prolactin secretion. Thus, it is possible that met-enkephalin released by the TIDA neurons during late pregnancy and lactation can directly enhance the secretory activity of the lactotrophs.

Collectively, these data reveal a remarkable plasticity in TIDA neurons during late pregnancy and lactation. We propose a model whereby chronically elevated placental lactogen modifies prolactin receptor signaling, leading to a reduction in ERK1/2-mediated phosphorylation of TH and a concurrent activation of met-enkephalin expression. The consequent reduction of dopamine synthesis means that, in response to continued stimulation by prolactin, these neurons alter their behavior and secrete met-enkephalin instead of dopamine. The met-enkephalin acts via opioid autoreceptors on the TIDA neurons, further suppressing the activity of TH. It may also travel in the portal blood to the pituitary, where it promotes prolactin secretion from the lactotrophs. These changes facilitate suckling-induced prolactin secretion by allowing it to be maintained unopposed by a negative feedback and indeed potentially facilitated by positive feedback actions. This adaptive switch in TIDA neuron behavior establishes a period of hyperprolactinemia that is only terminated by the weaning of the pups.

STAR★METHODS

Detailed methods are provided in the online version of this paper and include the following:

- KEY RESOURCES TABLE
- CONTACT FOR REAGENT AND RESOURCE SHARING
- EXPERIMENTAL MODEL AND SUBJECT DETAILS
  - Genetic mouse models
- METHOD DETAILS
  - Immunohistochemistry
  - Western blotting
  - Quantitative PCR
  - *In situ* hybridization for Penk mRNA
  - *In vitro* measurement of met-enkephalin and TH expression in the median eminence
  - Two-photon multicellular Ca^{2+} imaging in the pituitary
- QUANTIFICATION AND STATISTICAL ANALYSIS

SUPPLEMENTAL INFORMATION

Supplemental Information includes two figures and can be found with this article online at https://doi.org/10.1016/j.celrep.2019.01.067.

ACKNOWLEDGMENTS

This work was funded by the Agence Nationale de la Recherche ANR-DAT-NET 2007 (to A.O.M.); France-BioImaging ANR-10-INBS-04 and ANR 12 BSV1 0032-01 (to P.M.); The Royal Society New Zealand, Marsden Fund UOO1406 (to S.J.B.) and New Zealand Heath Research Council Program Grant 14-568 (to D.R.G.); Diabetes UK R.D. Lawrence (12/0004431) Fellowship; and MRC (MR/N00275X/1) Project and Diabetes UK (17/0005681) Project Grants (to D.J.H.). This project has received funding from the European Research Council (ERC) under the European Union's Horizon 2020 research and innovation programme (starting grant 715884 to D.J.H.).

AUTHOR CONTRIBUTIONS

Conceptualized, P.M., D.R.G., and S.J.B.; Methodology, S.H.Y., P.M., D.R.G., and S.J.B.; Investigation, S.H.Y., N.R., D.J.H., E.J.W., P.G., I.C.K., and P.M.; Writing – Original Draft, S.H.Y. and S.J.B.; Writing – Review and Editing, N.R., D.J.H., S.H.Y., A.O.M., P.M., and D.R.G.; Funding Acquisition, P.M., A.O.M., D.R.G., S.J.B., and D.J.H.; Supervision, P.M., A.O.M., D.R.G., and S.J.B.

DECLARATION OF INTERESTS

The authors declare no competing interests.

Received: January 25, 2018
Revised: September 27, 2018
Accepted: January 16, 2019
Published: February 12, 2019

REFERENCES

Andrews, Z.B. (2005). Neuroendocrine regulation of prolactin secretion during late pregnancy: easing the transition into lactation. J. Neuroendocrinol. *17*, 466–473.

Andrews, Z.B., and Grattan, D.R. (2002). Opioid control of prolactin secretion in late pregnant rats is mediated by tuberoinfundibular dopamine neurons. Neurosci. Lett. *328*, 60–64.

Arbogast, L.A., and Voogt, J.L. (1996). The responsiveness of tuberoinfundibular dopaminergic neurons to prolactin feedback is diminished between early lactation and midlactation in the rat. Endocrinology *137*, 47–54.

Arbogast, L.A., and Voogt, J.L. (1998). Endogenous opioid peptides contribute to suckling-induced prolactin release by suppressing tyrosine hydroxylase activity and messenger ribonucleic acid levels in tuberoinfundibular dopaminergic neurons. Endocrinology *139*, 2857–2862.

Arita, J.A., and Kimura, K. (1988). Enkephalin inhibits dopamine synthesis in vitro in the median eminence portion of rat hypothalamic slices. Endocrinology *123*, 694–699.

Augustine, R.A., Kokay, I.C., Andrews, Z.B., Ladyman, S.R., and Grattan, D.R. (2003). Quantitation of prolactin receptor mRNA in the maternal rat brain during pregnancy and lactation. J. Mol. Endocrinol. *31*, 221–232.

Battaglia, A.A., Beltramo, M., Thibault, J., Krieger, M., and Calas, A. (1995). A confocal approach to the morphofunctional characterization of the transient tyrosine hydroxylase system in the rat suprachiasmatic nucleus. Brain Res. *696*, 7–14.

Berghorn, K.A., Le, W.W., Sherman, T.G., and Hoffman, G.E. (2001). Suckling stimulus suppresses messenger RNA for tyrosine hydroxylase in arcuate neurons during lactation. J. Comp. Neurol. *438*, 423–432.

Bernichtein, S., Touraine, P., and Goffin, V. (2010). New concepts in prolactin biology. J. Endocrinol. *206*, 1–11.

Brisken, C., Kaur, S., Chavarria, T.E., Binart, N., Sutherland, R.L., Weinberg, R.A., Kelly, P.A., and Ormandy, C.J. (1999). Prolactin controls mammary gland development via direct and indirect mechanisms. Dev. Biol. *210*, 96–106.

Brown, R.S., Kokay, I.C., Herbison, A.E., and Grattan, D.R. (2010). Distribution of prolactin-responsive neurons in the mouse forebrain. J. Comp. Neurol. *518*, 92–102.

Brown, R.S., Herbison, A.E., and Grattan, D.R. (2011). Differential changes in responses of hypothalamic and brainstem neuronal populations to prolactin during lactation in the mouse. Biol. Reprod. *84*, 826–836.

Brown, R.S., Piet, R., Herbison, A.E., and Grattan, D.R. (2012). Differential actions of prolactin on electrical activity and intracellular signal transduction in hypothalamic neurons. Endocrinology *153*, 2375–2384.

Brown, R.S., Kokay, I.C., Phillipps, H.R., Yip, S.H., Gustafson, P., Wyatt, A., Larsen, C.M., Knowles, P., Ladyman, S.R., LeTissier, P., and Grattan, D.R. (2016). Conditional deletion of the prolactin receptor reveals functional subpopulations of dopamine neurons in the arcuate nucleus of the hypothalamus. J. Neurosci. *36*, 9173–9185.

Brunton, P.J., Russell, J.A., and Douglas, A.J. (2008). Adaptive responses of the maternal hypothalamic-pituitary-adrenal axis during pregnancy and lactation. J. Neuroendocrinol. *20*, 764–776.

Callahan, P., Klosterman, S., Prunty, D., Tompkins, J., and Janik, J. (2000). Immunoneutralization of endogenous opioid peptides prevents the suckling-induced prolactin increase and the inhibition of tuberoinfundibular dopaminergic neurons. Neuroendocrinology *71*, 268–276.

Campbell, J.N., Macosko, E.Z., Fenselau, H., Pers, T.H., Lyubetskaya, A., Tenen, D., Goldman, M., Verstegen, A.M., Resch, J.M., McCarroll, S.A., et al. (2017). A molecular census of arcuate hypothalamus and median eminence cell types. Nat. Neurosci. *20*, 484–496.

Carretero, J., Blanco, E., Sánchez, F., Riesco, J.M., Rubio, M., Juanes, J.A., and Vázquez, R. (1992). Morphometrical variations of prolactin cells in response to prolonged and systemic administration of Met-enkephalin in female rats. Anat. Embryol. (Berl.) *186*, 99–105.

Carretero, J., Bodego, P., Rodríguez, R.E., Rubio, M., Blanco, E., and Burks, D.J. (2004). Expression of the mu-opioid receptor in the anterior pituitary gland is influenced by age and sex. Neuropeptides *38*, 63–68.

Chihara, K., Arimura, A., Chihara, M., and Schally, A.V. (1978). Studies on the mechanism of growth hormone and thyrotropin responses to somatostatin antiserum in anesthetized rats. Endocrinology *103*, 1916–1923.

Ciofi, P., Crowley, W.R., Pillez, A., Schmued, L.L., Tramu, G., and Mazzuca, M. (1993). Plasticity in expression of immunoreactivity for neuropeptide Y, enkephalins and neurotensin in the hypothalamic tubero-infundibular dopaminergic system during lactation in mice. J. Neuroendocrinol. *5*, 599–602.

Demarest, K.T., McKay, D.W., Riegle, G.D., and Moore, K.E. (1983). Biochemical indices of tuberoinfundibular dopaminergic neuronal activity during lactation: a lack of response to prolactin. Neuroendocrinology *36*, 130–137.

Enjalbert, A., Ruberg, M., Arancibia, S., Priam, M., and Kordon, C. (1979). Endogenous opiates block dopamine inhibition of prolactin secretion in vitro. Nature *280*, 595–597.

Ferland, L., Fuxe, K., Eneroth, P., Gustafsson, J.A., and Skett, P. (1977). Effects of methionine-enkephalin on prolactin release and catecholamine levels and turnover in the median eminence. Eur. J. Pharmacol. *43*, 89–90.

Freeman, M.E., Kanyicska, B., Lerant, A., and Nagy, G. (2000). Prolactin: structure, function, and regulation of secretion. Physiol. Rev. *80*, 1523–1631.

Grattan, D.R. (2015). 60 years of endocrinology: the hypothalamo-prolactin axis. J. Endocrinol. *226*, T101–T122.

Grattan, D.R., and Kokay, I.C. (2008). Prolactin: a pleiotropic neuroendocrine hormone. J. Neuroendocrinol. *20*, 752–763.

Grattan, D.R., and Le Tissier, P. (2015). Hypothalamic Control of Prolactin Secretion, and the Multiple Reproductive Functions of Prolactin. In Knobil and Neill's Physiology of Reproduction, Fourth Edition (Academic Press), pp. 469–526.

Grattan, D.R., Steyn, F.J., Kokay, I.C., Anderson, G.M., and Bunn, S.J. (2008). Pregnancy-induced adaptation in the neuroendocrine control of prolactin secretion. J. Neuroendocrinol. *20*, 497–507.

Gustafson, P., Kokay, I., Sapsford, T., Bunn, S., and Grattan, D. (2017). Prolactin regulation of the HPA axis is not mediated by a direct action upon CRH neurons: evidence from the rat and mouse. Brain Struct. Funct. *222*, 3191–3204.

He, Z., Fernandez-Fuente, M., Strom, M., Cheung, L., Robinson, I.C., and Le Tissier, P. (2011). Continuous on-line monitoring of secretion from rodent pituitary endocrine cells using fluorescent protein surrogate markers. J. Neuroendocrinol. *23*, 197–207.

Hodson, D.J., Schaeffer, M., Romanò, N., Fontanaud, P., Lafont, C., Birkenstock, J., Molino, F., Christian, H., Lockey, J., Carmignac, D., et al. (2012). Existence of long-lasting experience-dependent plasticity in endocrine cell networks. Nat. Commun. *3*, 605.

Kokay, I.C., and Grattan, D.R. (2005). Expression of mRNA for prolactin receptor (long form) in dopamine and pro-opiomelanocortin neurones in the arcuate nucleus of non-pregnant and lactating rats. J. Neuroendocrinol. *17*, 827–835.

Kumer, S.C., and Vrana, K.E. (1996). Intricate regulation of tyrosine hydroxylase activity and gene expression. J. Neurochem. *67*, 443–462.

Larsen, C.M., and Grattan, D.R. (2012). Prolactin, neurogenesis, and maternal behaviors. Brain Behav. Immun. *26*, 201–209.

Liang, S.L., and Pan, J.T. (2011). The spontaneous firing rates of dopamine-inhibited dorsomedial arcuate neurons exhibit a diurnal rhythm in brain slices obtained from ovariectomized plus estrogen-treated rats. Brain Res. Bull. *85*, 189–193.

Lyons, D.J., Horjales-Araujo, E., and Broberger, C. (2010). Synchronized network oscillations in rat tuberoinfundibular dopamine neurons: switch to tonic discharge by thyrotropin-releasing hormone. Neuron *65*, 217–229.

Lyons, D.J., Hellysaz, A., and Broberger, C. (2012). Prolactin regulates tuberoinfundibular dopamine neuron discharge pattern: novel feedback control mechanisms in the lactotrophic axis. J. Neurosci. *32*, 8074–8083.

Magoul, R., Dubourg, P., Benjelloun, W., and Tramu, G. (1993). Direct and indirect enkephalinergic synaptic inputs to the rat arcuate nucleus studied by combination of retrograde tracing and immunocytochemistry. Neuroscience *55*, 1055–1066.

Magoul, R., Dubourg, P., Kah, O., and Tramu, G. (1994). Ultrastructural evidence for synaptic inputs of enkephalinergic nerve terminals to target neurons in the rat arcuate nucleus. Peptides *15*, 883–892.

Mansour, A., Thompson, R.C., Akil, H., and Watson, S.J. (1993). Delta opioid receptor mRNA distribution in the brain: comparison to delta receptor binding and proenkephalin mRNA. J. Chem. Neuroanat. *6*, 351–362.

Meltzer, H.Y., Miller, R.J., Fessler, R.G., Simonovic, M., and Fang, V.S. (1978). Effects of enkephalin in analogues on prolactin release in the rat. Life Sci. *22*, 1931–1937.

Merchenthaler, I. (1994). Induction of enkephalin in tuberoinfundibular dopaminergic neurons of pregnant, pseudopregnant, lactating and aged female rats. Neuroendocrinology *60*, 185–193.

Merchenthaler, I., Lennard, D.E., Cianchetta, P., Merchenthaler, A., and Bronstein, D. (1995). Induction of proenkephalin in tuberoinfundibular dopaminergic neurons by hyperprolactinemia: the role of sex steroids. Endocrinology *136*, 2442–2450.

Nahi, F., and Arbogast, L.A. (2003). Prolactin modulates hypothalamic preproenkephalin, but not proopiomelanocortin, gene expression during lactation. Endocrine *20*, 115–122.

Rivier, C., Vale, W., Ling, N., Brown, M., and Guillemin, R. (1977). Stimulation in vivo of the secretion of prolactin and growth hormone by beta-endorphin. Endocrinology *100*, 238–241.

Romanò, N., Yip, S.H., Hodson, D.J., Guillou, A., Parnaudeau, S., Kirk, S., Tronche, F., Bonnefont, X., Le Tissier, P., Bunn, S.J., et al. (2013). Plasticity of hypothalamic dopamine neurons during lactation results in dissociation of electrical activity and release. J. Neurosci. *33*, 4424–4433.

Romanov, R.A., Zeisel, A., Bakker, J., Girach, F., Hellysaz, A., Tomer, R., Alpár, A., Mulder, J., Clotman, F., Keimpema, E., et al. (2017). Molecular interrogation of hypothalamic organization reveals distinct dopamine neuronal subtypes. Nat. Neurosci. *20*, 176–188.

Spitzer, N.C. (2017). Neurotransmitter switching in the developing and adult brain. Annu. Rev. Neurosci. *40*, 1–19.

Stagkourakis, S., Kim, H., Lyons, D.J., and Broberger, C. (2016). Dopamine autoreceptor regulation of a hypothalamic dopaminergic network. Cell Rep. *15*, 735–747.

Szabó, F.K., Le, W.W., Snyder, N.S., and Hoffman, G.E. (2011). Comparison of the temporal programs regulating tyrosine hydroxylase and enkephalin expressions in TIDA neurons of lactating rats following pup removal and then pup return. J. Mol. Neurosci. *45*, 110–118.

Tavakoli-Nezhad, M., and Arbogast, L.A. (2010). Mu and kappa opioid receptor expression in the mediobasal hypothalamus and effectiveness of selective antagonists on prolactin release during lactation. Neuroscience *166*, 359–367.

Ugrumov, M.V. (2009). Non-dopaminergic neurons partly expressing dopaminergic phenotype: distribution in the brain, development and functional significance. J. Chem. Neuroanat. *38*, 241–256.

Wang, H.J., Hoffman, G.E., and Smith, M.S. (1993). Suppressed tyrosine hydroxylase gene expression in the tuberoinfundibular dopaminergic system during lactation. Endocrinology *133*, 1657–1663.

Zhang, X., and van den Pol, A.N. (2015). Dopamine/tyrosine hydroxylase neurons of the hypothalamic arcuate nucleus release GABA, communicate with dopaminergic and other arcuate neurons, and respond to dynorphin, met-enkephalin, and oxytocin. J. Neurosci. *35*, 14966–14982.

STAR★METHODS

KEY RESOURCES TABLE

REAGENT or RESOURCE	SOURCE	IDENTIFIER
Antibodies		
Rabbit polyclonal anti-methionine-enkephalin	ImmunoStar	Cat#20065; RRID:AB_572250
Rabbit polyclonal anti-tyrosine hydroxylase	Millipore	Cat#AB151; RRID:AB_10000323
Mouse monoclonal anti-tyrosine hydroxylase	Millipore	Cat# MAB318, RRID:AB_2201528
Rabbit monoclonal anti-phospho-Stat5 (Tyr694) (C11C5)	Cell Signaling Technology	Cat#9359; RRID:AB_823649
Rabbit polyclonal anti-human/mouse STAT5a/b pan specific affinity purified PAb	R & D Systems	Cat# AF2168, RRID:AB_355174
Rabbit monoclonal anti-phospho-p44/42 MAPK (Erk1/2) (Thr202/Tyr204)	Cell Signaling Technology	Cat# 4370, RRID:AB_2315112
Rabbit monoclonal anti-p44/42 MAPK (Erk1/2) (137F5)	Cell Signaling Technology	Cat# 4695, RRID:AB_390779
Rabbit polyclonal anti-phospho-tyrosine hydroxylase (Ser40)	Thermo Fisher Scientific (Zymed)	Cat# 36-8600, RRID:AB_138590
Mouse monoclonal anti-beta actin (clone mAbcam)	Abcam	Cat#ab8226, RRID:AB_306371
Rabbit anti-oPRL-2	NIDDK	Cat#AFP-C358106
Rabbit-mPRL	NIDDK	Cat#AFP-C131078
Goat polyclonal anti-mouse IgG (H+L) (AffiniPure Fab Fragment)	Jackson ImmunoResearch Lab	Cat# 115-007-003; RRID: AB_2338476
Goat polyclonal anti-rabbit BiotinX IgG (H+L) (Biotin-XX conjugated)	Thermo Fisher Scientific	Cat# B2770, RRID:AB_10375717
Goat anti-mouse IgG (H+L) (Alexa Fluor 488 conjugated)	Molecular Probes	Cat# A-11029, RRID:AB_138404
Goat anti-rabbit IgG (H+L) (Alexa Fluor 568 conjugated)	Molecular Probes	Cat# A-11036, RRID:AB_143011
Sheep anti-digoxigenin (alkaline phosphatase conjugated)	Roche	Cat# 11093274910 RRID: AB_514497
Chemicals, Peptides, and Recombinant Proteins		
Bromocriptine mesylate	Tocris Bioscience	Cat#0427; CAS: 22260-51-1
Ovine prolactin from sheep pituitary	Sigma-Aldrich	L6520-250IU; CAS: 9002-62-4
Colchicine	Sigma-Aldrich	C9754-100MG; CAS: 64-86-8
Ovine PRL-1-3	NIDDK	Cat#AFP-10789D
Mouse PRL	NIDDK	Cat#AFP-9038E
Fura-2 LR	TEFlabs	No longer available
Methionine-enkephalin	Sigma-Aldrich	M6638; CAS: 82362-17-2
Critical Commercial Assays		
RNeasy Mini Kit	QIAGEN	Cat#74104
Riboprobe *in vitro* transcription kit	Promega	Cat#P1460
SuperScript III reverse transcriptase	Invitrogen	Cat#180800-51
Pierce BCA Protein Assay Kit	Thermo Scientific	Cat#23227
Experimental Models: Organisms/Strains		
Mouse: $PRLR^{lox/lox}$/CamK-Cre	Brown et al., 2016	N/A
Mouse: PRL-DsRed	He et al., 2011	N/A
Oligonucleotides		
Primer for *Penk,* forward (qPCR): TCCTGAGGCTTTGCACCTGG	This paper	NM_001002927.2
Primer for *Penk,* reverse (qPCR) AGTGTGCAGCCAGGAAATTG-3	This paper	NM_001002927.2
Primer for *Penk,* forward (ISH): CTTTGCACCTGGCTGCTGGC	This paper	NM_001002927.2
Primer for *Penk,* reverse (ISH): GGGAACTCGGGCCTGGACAC (ISH)	This paper	NM_001002927.2
Primer for TH, forward: GCCCCCAGAGATGCAAGTC	This paper	NM_009377.1

(*Continued on next page*)

Continued		
REAGENT or RESOURCE	SOURCE	IDENTIFIER
Primers for TH, reverse: GCCTGGATGGCTACGTACATCATG	This paper	NM_009377.1
Primers for beta-actin, forward: ATGGGGCCAGGAGAAATCTA	This paper	NM_007393.3
Primers for beta-actin, reverse: GCCTGGATGGCTACGTACATCATG	This paper	NM_007393.3
Software and Algorithms		
R-projects, custom scripts	This paper	https://www.r-project.org/
PRISM Version 7.0	GraphPad Software, San Diego, USA	https://www.graphpad.com/
AssayZap Version 3.0	Biosoft Cambridge, UK	http://www.biosoft.com/w/assayzap.htm
ImageJ	Gustafson et al., 2017	https://imagej.nih.gov/ij/
Quantity One 1-D Analysis	Bio-Rad	http://www.bio-rad.com
Other		
Micro-osmotic pump Model 1003D	Alzet; Durect Corporation	Cat#0000289

CONTACT FOR REAGENT AND RESOURCE SHARING

Further information and requests for resources and reagents should be directed to and will be fulfilled by the Lead Contact, Stephen Bunn, (stephen.bunn@otago.ac.nz).

EXPERIMENTAL MODEL AND SUBJECT DETAILS

Genetic mouse models

Generation of PRLR$^{lox/lox}$/CamK-Cre mice

A conditional transgenic mouse was also used in which prolactin receptors had been deleted from most forebrain neurons, including TIDA neurons, by crossing homozygous female prolactin receptor flox mice (PRL-R$^{lox/lox}$) with heterozygous male CamKinase IIα Cre-recombinase mice (Brown et al., 2016). In brief, the presence of the wild-type Prlr allele was detected by primer 1 (5′-TGT CCA GAC TAC AAA ACC AGT GGC-3′) and primer 2 (5′-CAG TGC TCT GGA GAG CTG GC-3′), which span the Lox71 site subsequent to exon 5 and amplify a 546 bp product from wild-type mice but not from Prlrlox/lox mice. Mice carrying a Prlr lox/lox allele were identified using primer 1 and primer 3 (5′-ACC TCC CCC TGA ACC TGA AAC ATA A-3′). Primer 3 is located within the inverted GFP sequence and thus only produces a ~400 bp band from mice heterozygous or homozygous for the Prlr lox/lox allele, whereas no band is generated from wild-type mice. The presence or absence of CamK-Cre was determined using primers creP1 (5′-GGT TCT CCG TTT GCA CTC AGG-3′), creP3 (5′-CTG CAT GCA CGG GAC AGC TCT-3′), and creP17 (5′-GCT TGC AGG TAC AGG AGG TAG T-3′). CreP1 and creP3 span the start site of the endogenous CaMKIIα gene locus and produce a 285 bp band in wild-type animals only. CreP17 anneals within the inserted cre sequence at the modified CaMKIIα-cre gene locus to generate a 380 bp product with creP1, but only in mice with at least one copy of this Cre construct.

Generation of prolactin-DsRed mouse

Transgenic mice expressing DSRed under the control of the prolactin promoter were generated as previous described in He et al. (2011) and Hodson et al. (2012).

Animal care and procedures

Animal procedures complied with the animal welfare guidelines of the European Community (Agreement 34.128) or the Animal Ethics Committee of the University of Otago. Adult virgin female mice aged 8-12 weeks and weighing 20-25 g were obtained from the University of Otago animal breeding facility, or for data presented in Figures 5 and 6, from Charles River (France). Animals were group housed under controlled temperature (22 ± 1°C) and lighting (12 h light, 12 h dark cycle, lights on at 0600 h) conditions with *ad libitum* access to food and water. Estrous cycles were monitored by daily cytological examination of vaginal smears with diestrous animals used as non-pregnant controls. Late-pregnant mice were used on day 18 of pregnancy, the presence of vaginal plug indicating day 1, and lactating mice were used between day 7 and 10 post-partum. In some experiments, endogenous prolactin secretion was suppressed by three consecutive injections of bromocriptine mesylate (5 mg/kg sc every 12 h, Sigma-Aldrich). Some animals were injected with ovine prolactin (10 mg/kg ip, Sigma-Aldrich) at the same time as the bromocriptine treatment. For investigation of prolactin action on intracellular signaling pathways, mice were injected with saline or ovine prolactin (10 mg/kg ip) 20 min prior to being perfused and processed for immunohistochemistry (see below). Immunohistochemical staining for met-enkephalin required animals to be treated with 30 μg colchicine (Sigma-Aldrich; 1 μL icv injection at Bregma +0.75 mm lateral, −0.1 mm posterior and +2.4 mm ventral) 24 h before perfusion. Serum levels of mouse prolactin were measured using radioimmunoassay as described previously (Brown et al., 2010). The effect of maintaining elevated prolactin concentrations in the absence of the suckling stimulus on

Penk mRNA expression was investigated using lactating mice which were without pups for 24 h. Prolactin levels were maintained in the absence of suckling by a subcutaneous osmotic minipump (1003D, Alzet™) delivering ovine prolactin (1500 μg/d in 0.01 M sodium bicarbonate buffer (pH 9.2); biopotency 20-50 IU, Sigma-Aldrich). Prolactin or vehicle (saline) filled pumps were implanted on days 4 to 6 of lactation under isoflurane anesthesia and the animals left to recover for 24 h. The pups were then removed and the dams left for a further 24 h before they were perfused with 2% PFA in 0.1 M phosphate buffer (pH 7.4). Atrial blood samples obtained immediately prior to perfusion were used for the measurement of plasma ovine prolactin concentrations by radioimmunoassay.

METHOD DETAILS

Immunohistochemistry

Animals were euthanized with 3 mg sodium pentobarbital, transcardially perfused with 4% paraformaldehyde and the brains excised and post-fixed in the same fixative for at least 1 h before being cryoprotected with 30% sucrose in Tris-buffered saline (TBS) at 4°C overnight. Four sets of 30 μm sections from the level of paraventricular nucleus (Bregma −0.58 mm) to caudal arcuate nucleus (Bregma −2.12 mm) were obtained. Immunostaining for either met-enkephalin or TH was achieved by incubating tissue sections, in which endogenous peroxidase activity had been quenched (0.1% H_2O_2:40% methanol in TBS), overnight at 4°C with either rabbit anti-methionine enkephalin (Immunostar, catalog #20065) or rabbit anti-TH (Millipore, catalog #AB151) diluted 1:1000 and 1:10000 respectively, in TBS containing 0.03% Triton-X, 0.25% bovine serum albumin and 2% normal goat serum. Sections were then incubated for 90 min at room temperature with biotinylated goat anti-rabbit IgG (Invitrogen; diluted 1:500) and staining visualized using biotin-avidin complex kit (Vector Laboratories) with nickel enhanced 3,3′-diaminobenzidine (DAB) (Sigma-Aldrich). Immunostaining for pSTAT5 required antigen retrieval (5 min in 10 mM Tris-HCl, pH 10 at 90°C followed by a further 5 min cooling at room temperature) and three 10 min washings in TBS (Brown et al., 2010). Endogenous peroxidase activity was then quenched as above and sections incubated for 72 h at 4°C with rabbit anti-pSTAT5 (Tyr694) (Cell Signaling Technology catalog #9359; diluted 1:400) followed by nickel-enhanced DAB detection as above. Dual-labeling these sections for TH was achieved by repeating the peroxidase quenching and then incubating overnight at 4°C with rabbit anti-TH (diluted as above) followed by peroxidase-conjugated goat anti-rabbit IgG (Vector Laboratories; diluted 1:200) and then DAB without nickel enhancement. Dual-labeling for TH with either met-enkephalin or pERK1/2 required the use of fluorescently-conjugated anti-mouse secondary antibodies. To achieve low background staining, endogenous mouse immunoglobulins were first blocked by incubating the sections overnight at 4°C with an AffiniPure Fab' fragment of goat anti-mouse IgG (H+L) (Jackson ImmunoResearch Laboratories, catalog #15-007-003; diluted 1:100 in TBS), followed by a cocktail of mouse anti-TH (Millipore, catalog #MAB318, diluted 1:1000) with anti-met-enkephalin (as above) or rabbit anti-phospho-pERK1/2, (Cell Signaling Technology, catalog #4370 diluted 1:1000) overnight at 4°C. Staining was visualized using the fluorescently-tagged secondary antibodies (Molecular Probes catalog #A11029 and #A11036, both diluted 1:1000). All DAB or fluorescently stained sections were mounted on gelatin-coated glass slides and coverslipped with DPX or Vectashield mounting medium, respectively. Stained sections were viewed and photographed using an Olympus BX51 microscope. Confocal images were captured using a Zeiss LSM 510 Meta upright confocal microscope with excitation at 488 nm and 543 nm and a z-interval of 5 μm. A positive-labeled cell was counted if it had the nucleus present with at least one proximal process visible and was of approximately 10-20 μm in diameter. Quantification was performed from 3-4 representative sections of dorsomedial arcuate nucleus, an anatomical location of the TIDA population (Lyons et al., 2010; Zhang and van den Pol, 2015). In Figure 1, the whole arcuate nucleus was analyzed to provide a more appropriate comparison to the qPCR data obtained from tissue punches.

Western blotting

For the data in Figure 5 mice injected (ip) with naloxone (10 mg/kg) or saline (day 10 of lactation) were killed by cervical dislocation and the brains immediately excised and frozen on dry ice before being stored at −80°C. Coronal sections (300 μm at approximately Bregma −1.46 to −2.12 mm) were cut on a cryostat and micropunched samples of the arcuate nucleus, prepared as described above but including the median eminence, were transferred to 30 μL of 50 mM Tris buffer containing 2 mM ethylenediaminetetraacetic acid, 10 mM NaF, 2 mM NaP_2O_7, 2 mM Na_2-glycerophosphate, 1 mM Na_3VO_4, 1 mM PMSF and 4% sodium lauryl sulfate. Protein concentrations were determined using a Pierce BCA kit. β-mercaptoethanol (8% final) was then added to the samples, which were heated to 100°C. Protein samples (10 μg) were separated by 7.5% sodium dodecyl sulfate-polyacrylamide gel electrophoresis and transferred to nitrocellulose membranes which were probed with antibodies against TH phosphorylated at Ser-40 (Zymed Laboratories, catalog #368600) diluted 1:2000 in TBS containing 0.3% Triton-X (Romanò et al., 2013). β-actin labeling was used as a loading control (Abcam, catalog #ab8226, diluted 1:12000). For the data presented in Figure S2 animals were treated with bromocriptine mesylate (5mg/kg) followed by 20 min of ovine prolactin (10 mg/ kg). For detection of phospho-proteins, antibodies against anti-pSTAT5 (Tyr694) (Cell Signaling Technology catalog #9359; diluted 1:1000) and anti-pERK1/2 (Cell Signaling Technology catalog #4370; diluted 1:12000) both diluted in TBST containing 5% BSA were used. The respective non-phospho proteins were detected with anti- STAT5a/b pan (R&D System catalog AF2168; diluted 1:1000) and anti-p44/42 MAPK (Cell Signaling Technology catalog #4695; diluted 1:6000) diluted in 5% non-fat milk in TBST and were used to normalize the levels of phospho-proteins. Immunoreactive bands were visualized using enhanced chemiluminescence detection in accordance with the manufacturer's instructions and densitometric analysis performed using Quantity One 1-D Analysis Software (Bio-Rad).

Quantitative PCR

Quantitative PCR was used to determine the level of mRNA expression in tissue samples micropunched from the arcuate nucleus. Mice were decapitated and their brains removed, frozen on dry-ice and stored at −80°C. Under RNase-free conditions, 300 μm coronal cryostat sections were prepared at approximately Bregma −1.34 to −2.30 mm and tissue punches collected from the arcuate nucleus using a blunt-end needle. A single 500 μm diameter punch was obtained from each section centered on the midline immediately superior to the median eminence. Punches from three consecutive sections were pooled in 350 μL of lysis buffer (RNeasy Mini Kit, QIAGEN) containing 1% β-mercaptoethanol. Following sonication, RNA was extracted using RNeasy mini spin columns (QIAGEN) and purity determined using a Nanodrop 2000 spectrophotometer (Life Technologies). All samples used in this study had a 260/280 nm ratio of 2 or greater. RNA aliquots (35 ng) were reverse transcribed using SuperScript III reverse transcriptase (Invitrogen) and stored at −20°C until required. Oligonucleotide primers for the following transcripts were designed using ensemble.org and Primer Blast. *Penk* (NM_001002927.2) forward: 5′-TCC TGA GGC TTT GCA CCT GG-3′, reverse: 5′-AGT GTG CAG CCA GGA AAT TG-3′); *Th* (NM_009377.1): forward: 5′-GCC CCC AGA GAT GCA AGT C-3′ and reverse: 5′-TGT TGG CTG ACC GCA CAT-3′ and *β-actin* (NM_007393.3), forward: 5′-ATG GGG CCA GGA GAA ATC TA-3′ and reverse: 5′-GCC TGG ATG GCT ACG TAC ATC ATG-3′ were used. SYBR green based qPCR was performed in triplicate using an Applied Biosystems ViiA7 qPCR system (Life Technologies) and the fold changes in mRNA levels determined by normalizing against β-actin mRNA using the ΔΔCt method. Primer efficiencies were confirmed to lie between 92 and 105%.

In situ hybridization for Penk mRNA

Animals were decapitated and coronal sections of 16 μm were obtained using a cryostat at −20°C and immediately mounted onto RNase free aminopropyltriethoxysilane (APS)-coated microscope slides. Slides mounted with brain sections were thawed at 55°C for 5 min before sections were fixed in 2% PFA (5 min). The slides were washed in 0.5 × sodium chloride citrate buffer (SCC; 75 mM sodium chloride, 7.5 mM sodium citrate, pH 7) prior to incubation in proteinase K (2 μg/ml and acetylation with 0.25% acetic anhydride). The slides were washed in 2 × SCC before being taken through graded ethanol incubations of increasing concentration before incubation in chloroform for 5 min. Slides were air-dried for 3 h. Primers were designed for the mouse *Penk* gene using the GenBank mRNA sequence (accession number NM 001002927.2). The sequences were:5′-CTTTGCACCTGGCTGCTGGC-3′(forward) *and* 5′-GGGAACTCGGGCCTGGACAC-3′ (reverse). Reverse transcription polymerase chain reaction (PCR) was used to generate a DNA template with sequences encoding the T7 and SP6 polymerase promoter sites incorporated onto the ends of the primer sequences. ^{35}S UTP-labeled RNA probes were transcribed from the cDNA template using a Riboprobe® *in vitro* transcription kit (Promega) and the appropriate polymerase (T7 for the antisense probe, SP6 for the sense probe). The probes were purified using Mini Quick spin columns (Roche) to remove unincorporated nucleotides. Probes were denatured at 95°C for 3 min (40 ng probe/slide with 50 μg tRNA/slide). Sections were then covered with 100 μl hybridization buffer/probe mix (hybridization buffer: 100 mM dithiothreitol, 0.3 M sodium chloride, 20 mM Tris base (pH 8), 5 mM EDTA, 1 × Denhardt's solution, 10% dextran sulfate, 50% formamide). The slides were coverslipped and incubated overnight at 55°C. Sections were washed, incubated with ribonuclease A (20 μg/ml) for 30 min and then washed in 0.1 × SCC (with 10 mM β-mercaptoethanol and 1 mM EDTA) at 55°C for 2 h. Sections were incubated with anti-digoxigenin (DIG) antibody conjugated to alkaline phosphatase (1:2000) for 48 h. The DIG-labeled probes were detected by NBT/BCIP (nitroblue tetrazolium chloride/5-bromo-4 chloro-3-indolyl-phosphate) substrate. Color development was monitored under the microscope. The reaction was terminated after 23 h by four 30 min washes in buffer (150 mM NaCl, 10 mM NaH2PO4, 1 mM EDTA). Sections were dipped in ethanol, dried at 42°C for 1 h, immersed in xylene and coverslipped with Vectamount mounting medium. No staining was evident in sections incubated with the sense probe. Images were captured using an Olympus BX61 light microscope fitted with a QImaging Micropublisher 5.0RTV camera (QImaging, Surrey, Canada). Quantification and analysis were performed as described previously (Gustafson et al., 2017)

In vitro measurement of met-enkephalin and TH expression in the median eminence

Lactating mice (day 10 of lactation) were killed by rapid decapitation, following isoflurane anesthesia. The brain was quickly removed and placed in ice-cold artificial cerebrospinal fluid (aCSF) containing 118 mM NaCl, 3 mM KCl, 11 mM D-glucose, 10 mM HEPES, 25 mM $NaHCO_3$, 6 mM $MgCl_2$ and 0.5 mM $CaCl_2$, osmolarity between 295 and 305 mOsm, pH 7.2 when gassed with 5% CO_2 and 95% O_2. The brain was then glued to the stage of a vibratome and 150 μm thick coronal sections cut and incubated in aCSF for 60 min at 37° in 5% CO_2/95% O_2. The medium was then replaced with another 500 μL of aCSF with or without ovine prolactin (500 ng/ml) and incubated for a further 30 min and then the tissue immersion fixed in 4% paraformaldehyde overnight. The next day, immunohistochemical detection of met-enkephalin and TH was performed, as described above. Slices were imaged on a Zeiss LSM 510 Meta confocal microscope and densitometric analysis performed using ImageJ.

Two-photon multicellular Ca^{2+} imaging in the pituitary

Ca^{2+} imaging was performed on pituitary slices from lactating mice (day 10) expressing DsRed under the control of the prolactin promoter as described previously (Hodson et al., 2012). Briefly, pituitaries were embedded in low melting point agarose (Invitrogen), before preparing slices (150 μm) using a vibrating microtome (Campden Instruments). Slices were then loaded for 1 h with 20 μM Fura-2 LR (TEFLabs) supplemented with pluronic acid (0.005%; Invitrogen). Multicellular Ca^{2+} imaging was performed using a TriM Scope (LaVision BioTec) coupled to an Olympus BX51 frame, 20x 0.95 NA water-dipping objective (Olympus) and

femtosecond-pulsed near-infrared laser (Coherent Chameleon) to produce two-photon excitation at λ = 780 nm (Fura-2) and λ = 970 nm (DsRed). Emitted signals were detected at λ = 525 ± 50 nm (Fura-2) and λ = 593 ± 40 nm (DsRed) using a 14-bit, 512 × 512 pixel back-illuminated EM-CCD camera (Andor). Slices were perfused at 36°C in a buffer containing 125 mM NaCl, 2.5 mM KCl, 1.25 mM NaH_2PO_4, 26 mM, $NaHCO_3$, 12 mM glucose, 2 mM $CaCl_2$ and 1 mM $MgCl_2$ with met-enkephalin (500 nM) added at the indicated time. A region of interest (ROI) was used to extract the intensity-over-time from Fura-2 loaded DsRed-positive cells (i.e., lactotrophs). Cells were manually triaged and only those responding to treatment considered for further analysis (33.9 ± 2.3%; 327/957 cells analyzed from 7 slices). Ca^{2+}-spiking frequency was measured in the responsive subpopulation using the Short-Time Fourier Transform and component frequencies plotted as a function of their power for each independent recording using 0.005 Hz bins to produce a power spectrum. Significance was determined for the frequency with the greatest power before, during and after treatment. All analysis was performed using custom scripts in R (R-Project) and results considered significant at $p < 0.05$.

QUANTIFICATION AND STATISTICAL ANALYSIS

All experiments were conducted on female mice. Unless otherwise stated, statistical analysis was performed using PRISM software (GraphPad). Individual tests and n values are reported in the Results and in the relevant figure legends. All data are presented as mean ± SEM per section. In all statistical tests, a value of $p < 0.05$ was accepted as significant. The number of TH and met-enkephalin immunoreactive cells in diestrus, late pregnant and lactating mice in Figure 1 was compared by one-way ANOVA followed by a Tukey's multiple comparison test with 4 to 5 animals per group. A one-way ANOVA was similarly used to compare levels of *Th* mRNA and *Penk* mRNA expression between these three groups. In Figure 1 the level co-expression of TH and met-enkephalin expression during diestrus and lactation were compared using an unpaired Student's t test with 3 to 4 animals per group. In Figure 2 the effect of altering prolactin levels on the number of cells expressing met-enkephalin was compared using one-way ANOVA followed by a Tukey's multiple comparison test with 5 to 8 animals per group. The number of *Penk* mRNA positive neurons between diestrous and lactating groups (Figure 2) was compared using unpaired Student's t test with 4 to 6 animals per group. The effect of prolactin after pup withdrawal on the number of *Penk* mRNA expressing cells was compared using unpaired Student's t test with 4 to 6 animals per group. In Figure 3 the effect of prolactin receptor deletion on the number of cells expressing met-enkephalin (3 animals per group) and the number of *Penk* mRNA positive cells (5 to 6 animals per group) was compared using two-way ANOVA followed by a Tukey's multiple comparison test with 3 animals per group. A two-way ANOVA, followed by a Tukey's multiple comparison test, was also used to compared the number of TH immunoreactive cells expressing pSTAT5 or pERK1/2, (Figure 4) with 3 to 6 animals per group. In Figure 5 an unpaired Student's t test was used to compare the relative level of met-enkephalin immunoreactivity in the median eminence and the relative levels of phosphorylated TH measure by western blot. The data obtained from Ca^{2+} imaging in Figure 6 was analyzed using custom scripts in R (R-Project).